Behavior of free and connected double-tee flanges reinforced with carbon-fiber-reinforced polymer

A. W. Botros, G. Lucier, S. H. Rizkalla, and H. Gleich

- This paper presents an experimental program conducted to evaluate the performance of precast concrete double-tee flanges reinforced with carbon-fiber-reinforced polymer grids under various types of loading.
- Test results indicated that the flanges were capable of resisting a maximum applied load significantly higher than their factored design loads and that the concentrated load-carrying capacity of the flange depends on the location of the applied load.
- Based on this investigation, idealized failure surfaces and the corresponding modes of failure were identified for the free and connected flanges of prestressed concrete double tees subjected to concentrated loads.

Precast, prestressed concrete double tees are typically used in parking structures and commercial buildings. Traditionally, the flanges of these members are reinforced with conventional steel reinforcement to carry the load in the transverse direction of the flange and to control shrinkage cracking and thermal stress. Although traditional steel reinforcement is safe and effective from a structural perspective, it is vulnerable to corrosion.

Recently, carbon-fiber-reinforced polymer (CFRP) grid has been used by several precast concrete producers to replace steel reinforcement in the flanges of double-tee members. The advantages of CFRP grid are a high strength-to-weight ratio, excellent resistance to corrosion, and ease of installation.

The use of CFRP materials in precast concrete members was led by the construction of several concrete highway bridges in Canada.[1,2] CFRP strands and bars were used as prestressing and shear reinforcement for the bridge girders. Part of the deck slab was also reinforced with CFRP. The long-term performance of the bridges was monitored using advanced sensing technologies, and no degradation has been observed in the CFRP after more than 15 years in service.

CFRP grid has also been used in the precast concrete industry as interwythe shear reinforcement in precast, prestressed concrete sandwich panels and has been inves-

tigated in several studies.[3–6] Test results from these studies indicated that a high degree of composite action can be achieved by using CFRP grids as shear connectors.

CFRP grids and bars have also been investigated as flexural reinforcement by Banthia et al.[7] who examined the behavior of concrete slabs reinforced with fiber-reinforced polymer (FRP) grids and conventional slabs reinforced with steel grids under vertical concentrated loads. The study investigated the influence of concrete strength. Test results indicated that the ultimate loads for the FRP-reinforced slabs were higher than those for the steel-reinforced slabs. Matthys and Taerwe[8] investigated the behavior of concrete slabs reinforced with FRP grids under concentrated loads. The study included testing steel-reinforced control slabs, slabs reinforced with CFRP grids, and slabs reinforced with a hybrid type of FRP that included both carbon and glass fibers. Other parameters were considered, such as slab depth and reinforcement ratio. Test results documented punching shear failures for most slabs. Punching strength for FRP-reinforced slabs was similar to or higher than that of the control slabs. A strong interaction between shear and flexural effects was also noted for most tested slabs.

El Gamal et al.[9] tested six full-scale deck slabs reinforced with glass-fiber-reinforced polymer (GFRP) and CFRP bars under a monotonic single concentrated load applied at the center of the slab. Three deck slabs were reinforced with GFRP bars, two deck slabs were reinforced with CFRP bars, and a reference slab was reinforced with steel. Test results indicated that all slabs, including the reference slab, were capable of resisting loads more than three times the design load specified by the *Canadian Highway Bridge Design Code*.[10]

Lunn et al.[11] tested eight 15 ft (4.6 m) wide and 10 ft (3 m) long double-tee beams with a flange thickness of 3.5 in. (89 mm). The study was conducted to evaluate the behavior, serviceability, and failure mode of double-tee flanges reinforced with CFRP grids under uniformly applied loads. The results of the study indicated that the proposed precast concrete double-tee beams reinforced with CFRP grids were capable of resisting uniform pressures well in excess of the design load. The mode of failure of the flanges was governed by the tensile strength of the concrete followed by rupture of the CFRP grid. The research proposed design recommendations for double-tee flanges reinforced with CFRP grids.

This current paper presents two experimental programs undertaken to examine the serviceability and failure mode of free and connected precast, prestressed concrete double-tee flanges reinforced with CFRP grids. Double-tee flanges were tested separately under uniformly distributed loads and under concentrated loads to evaluate the behavior of the flanges under extreme loading conditions.

Uniform load tests

Two full-scale double-tee specimens, each 12 × 40 ft (3.7 × 12 m), were tested under uniform loading. Specimen DT1 was a 28 in. (710 mm) deep untopped member with a 2 in. (50 mm) thick flange. Specimen DT1 would normally be field topped with reinforced concrete, so tests of specimen DT1 simulate the construction-loading condition with the wet topping applied. Specimen DT2 was a 29.5 in. (750 mm) deep pretopped member with a 3.5 in. (89 mm) thick flange. Specimen DT2 would normally be installed without additional composite field topping and would thus be directly subjected to final service conditions. Each specimen was prestressed longitudinally by ten ½ in. (13 mm) diameter special strands and reinforced for shear at the ends of each stem with steel welded-wire reinforcement. The specified nominal compressive strength of the concrete was 6000 psi (41 MPa), while the measured compressive strength at day of testing was 7000 psi (48 MPa). A continuous sheet of C25 FRP grid was used as the only transverse flange reinforcement. This grid comprised 0.15 in. (3.8 mm) wide carbon fiber strands spaced at 2.3 in. (58 mm) in the primary (transverse) direction, held together by smaller carbon-fiber strands crossing in the orthogonal direction. The primary CFRP strands provided the structural flange reinforcement, and the cross strands maintained spacing and provided anchorage for the primary grid strands. The cross strands also provided limited flange reinforcement in the longitudinal direction for temperature and shrinkage. Four individual carbon-fiber primary strands were cut from the grid and were tested to determine the maximum tensile strength. The strands exhibited an average tensile strength of 625 lb (2780 N).

The double-tee specimens were tested on a simple span using a vacuum chamber and air pressure to apply the uniform load. At one end of each specimen, the two stems were placed on two load cells, acting as a pin connection. At the other end, the two stems were placed on a 2 in. (50 mm) diameter cylindrical bar to provide a roller support. The specimen, supports, and instrumentation were enclosed in a vacuum chamber constructed around the specimen. The uniformly distributed load was applied on the top surface of the double-tee deck by reducing the pressure inside the chamber using a combination of vacuum equipment. **Figure 1** shows an isometric view of the test setup.

Figure 2 shows a cross section of the test setup and the concept used to apply a uniform pressure loading condition to the top surface of the flange. At the start of the test, pressures P1 and P2 were both equal to the atmospheric pressure. Consequently, no load was applied to the top surface of the double-tee deck. With the chamber sealed, pressure P2 was reduced with vacuum equipment while atmospheric pressure P1 remained constant. With pressure P1 greater than P2, the atmospheric pressure acted evenly

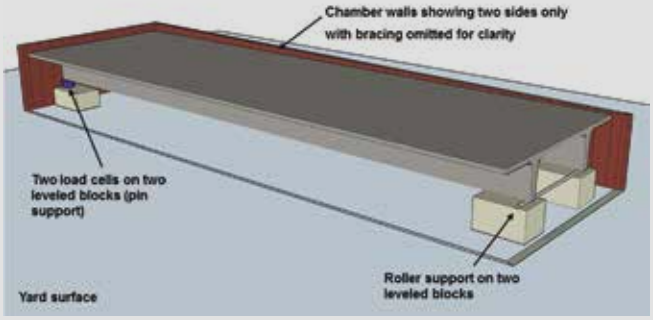

Figure 1. Test setup for double-tee specimens.

inward on the top surface of the double tee, creating a uniform downward pressure on the entire top surface of the flange.

Modular formwork panels were used to construct the four vertical walls of the chamber around each double tee. The panels were sealed to the pavement surface and wrapped in plastic to minimize air leakage. The chamber walls were also anchored to the pavement for stability and were braced against one another with shoring to resist the horizontal pressures acting on the chamber. Bracing was provided along the length of the chamber at the top and bottom of the sidewalls. The end walls were braced at the bottom against the supporting concrete blocks and were stiffened at their top edges with steel angles. The chamber was constructed with windows on all sides to allow access for instrumentation and for observation of the behavior under the applied load. Figure 2 shows the chamber under construction and the completed chamber before testing.

The total applied uniform pressure was monitored by pressure transducers and by load cells measuring the stem performance. The performance of the flanges was monitored at selected load levels for each specimen, including the design load. Specimen DT1, the untopped specimen, was designed for a dead load *DL* of 38 lb/ft^2 (1.8 kPa), representing a 2 in. (50 mm) field topping that would normally be applied. In addition, specimen DT1 was designed for a 10 lb/ft^2 (0.48 kPa) construction live load *LL*. Specimen DT2, the pretopped specimen, was designed for a live load of 40 lb/ft^2 (1.9 kPa) and a snow load *SL* of 20 lb/ft^2 (0.96 kPa). The controlling load case considered for both specimens was the factored load combination 1.2*DL* +

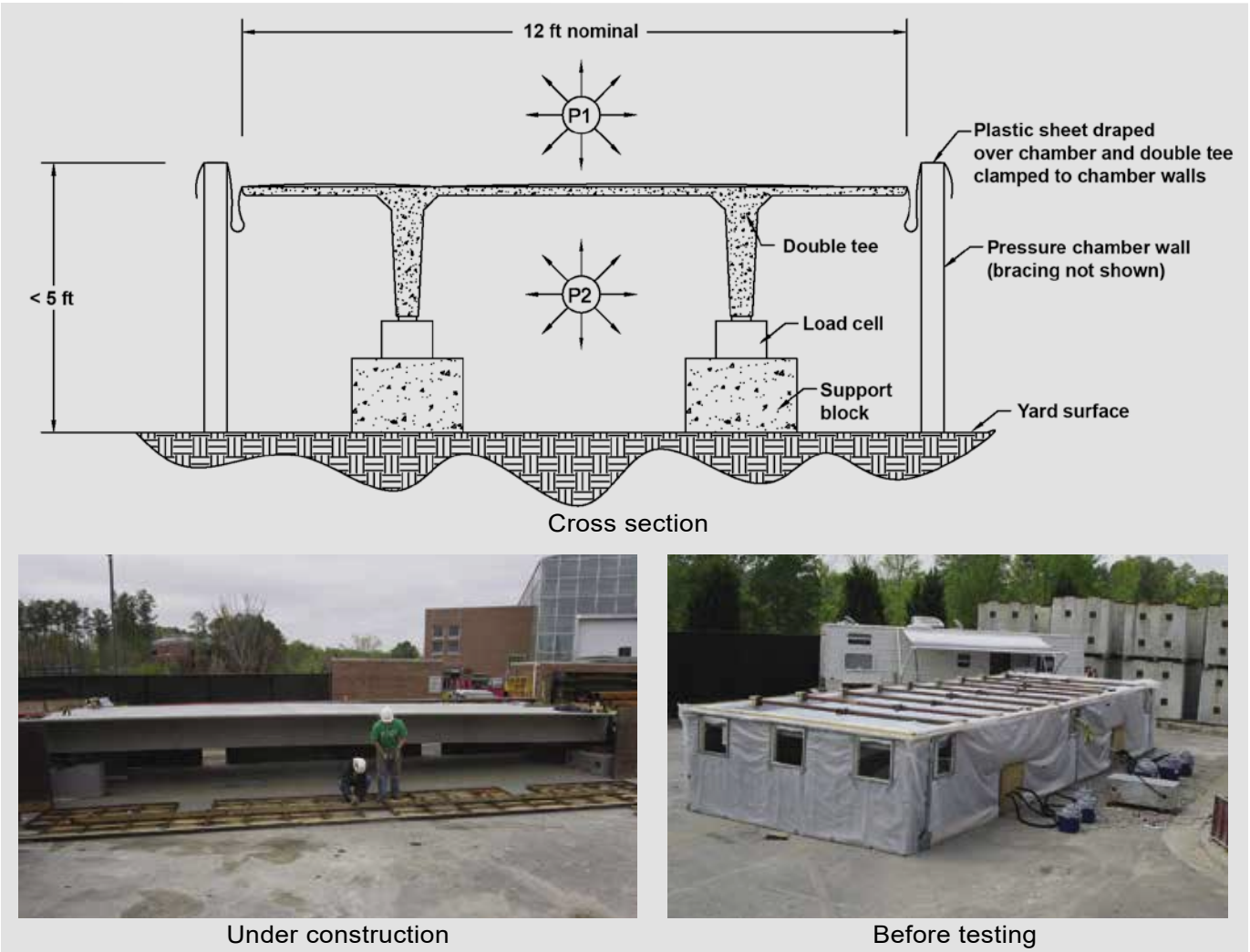

Figure 2. Sketch and photos of test chamber. Note: 1 ft = 0.305 m.

Table 1. Loading sequence for specimens DT1 and DT2

Specimen	Load step	Description	Applied pressure, lb/ft²	Applied stem reaction, lb	Total stem reaction, lb	Unload after step
DT1	0	Self-weight	0	0	5600	n/a
	1	*DL* topping	38	4560	10,160	Yes
	2	*DL* topping + *LL*	48	5760	11,360	Yes
	3	1.2*DL* + 1.6*LL*	66.6	7990	13,590	1 hour
	4	Increase to failure				
DT2	0	Self-weight	0	0	8400	n/a
	1	Applied *SL*	20	2400	10,800	Yes
	2	*LL* (service)	40	4800	13,200	Yes
	3	2 × flange weight	43.75	5250	13,650	Yes
	4	*LL* + *SL*	60	7200	15,600	Hold then continue
	6	1.2*DL* + 1.6*L* + 0.5*SL*	82.75	9930	18,330	Hold 24 hours, unload
	7	Recovery	0	0	8400	n/a
	8	90 lb/ft²	90	10,800	19,200	Yes
	9	100 lb/ft²	100	12,000	20,400	Yes
	10	110 lb/ft²	110	13,200	21,600	Yes
	11	120 lb/ft²	120	14,400	22,800	Yes
	14	Continue incremental loading to failure				

Note: *DL* = dead load; *LL* = live load; n/a = not applicable; *SL* = snow load. 1 lb = 4.448 N; 1 lb/ft² = 0.0479 kPa.

1.6*LL* + 0.5*SL*. The relevant factored load was sustained for 1 hour on specimen DT1 and for 24 hours on specimen DT2. The specimens were then loaded and unloaded in incremental cycles to failure. **Table 1** summarizes the loading sequences followed for the tests of specimens DT1 and DT2.

Six standard shop vacuums were used to generate pressures corresponding to the lower load steps. A vacuum excavation truck was used in addition to the shop vacuums to increase the applied pressure when needed for the higher load levels. A sliding gate was constructed to control the applied pressure. The gate was closed slowly to increase the differential pressure between the atmosphere and the chamber, consequently increasing the uniform load applied to the specimen.

Deflections, strains, and loads were monitored throughout testing. All instruments were connected to an electronic data acquisition system, which recorded data at 1 Hz during loading and unloading. String potentiometers were used to measure vertical displacements in lines along the width of the flange at the support, quarter-span, and midspan. Linear potentiometers were used to measure concrete strains on the top surface of the double tee. Thermocouples were used to measure the temperatures of the concrete surface during one test, and a pressure transducer was used to measure the internal chamber pressure. A U-tube differential manometer was also used for visual measurement of the pressure and to verify the electronically recorded pressures.

Test results and discussion

Both specimens DT1 and DT2 were capable of resisting loads exceeding their factored design loads before failure with minimal residual deflections after unloading. Test results for specimens DT1 and DT2 indicated that the flanges were able to resist a maximum uniform load equal to 1.3 times and more than 1.9 times their full factored design loads, respectively. **Table 2** gives the measured failure loads, including self-weight, for specimens DT1 and DT2. The performance of specimen DT2 is judged acceptable and the performance of specimen DT1 is judged unacceptable (despite the failure load substantially exceeding the factored load), as will be discussed later in this section.

Specimen DT1, with a 2 in. (50 mm) thick flange, failed at an applied pressure of 91 lb/ft² (4.3 kPa). The failure

Table 2. Ultimate loads for specimens DT1 and DT2

Load level	Total load resisted by flange, lb/ft²	
	DT1	DT2
Self-weight of flange	25	43.8
Service load (*DL* + *LL*)	73	83.8
Factored load (1.2*DL* + 1.6*LL* + 0.5S*L*)	91.6	126.6
Failure*	115.6	246.8
Failure load/service load	1.6	2.9*
Failure load/factored load	1.3	1.9*

Note: *DL* = dead load; *LL* = live load; *SL* = snow load. 1 lb/ft² = 0.0479 kPa.
*Specimen DT2 flange did not fail. The test was terminated with a significantly nonlinear load-deflection behavior at midspan.

mode was a flexural failure in one of the cantilever flanges of the beam accompanied by rupture of the CFRP grid reinforcement. The failure resulted in complete detachment of the cantilever flange along the entire length of the beam (**Fig. 3**). Failure occurred suddenly after the formation of a longitudinal flexural crack on the top surface of the flange. This crack was located 6.5 in. (165 mm) outward from the center of one stem where the flange tapered into the stem (Fig. 3). Two initial cracks on the top surface of the inner flange were observed in specimen DT1 before testing. The initial longitudinal cracks were located at the web-flange juncture and extended along the entire length of the beam. They were also visible on the bottom face of the flange but were not involved in the final failure mode.

Figures 4 and **5** show the measured net deflection profile at midspan and selected strain measurements for specimen DT1. Deflection profiles are shown at the service load, factored load, and ultimate load levels. The measured deflections at the tips of the cantilevers at service and factored loads were each less than 0.3 in. (8 mm). The measured transverse strains, gauges 2 and 4, located on the top surface of the cantilever at the flange stem juncture, indicated a linear load-strain behavior beyond the factored load and up to failure. This behavior indicates that no cracks occurred at this location up to failure. The behavior also justifies the small measured deflections at failure and highlights the brittle nature of failure. This result indicates that flange failure occurred immediately after cracking of the cross section at the maximum moment location. The load-strain behavior recorded by strain gauges 1 and 3 across the precracked inner flange-stem connection was nonlinear (Fig. 5). This result reflects widening of the preexisting cracks and straining of the CFRP grid at these locations as the applied uniform pressure increased.

Specimen DT2, with a 3.5 in. (89 mm) thick flange, did not exhibit a flange failure under the applied load. It exhibited global flexural deflections at midspan that had transitioned into the nonlinear stage, indicating yielding of the primary flexural reinforcement, at an applied load of 203 lb/ft² (9.72 kPa). The test of DT2 was terminated at this load level due to steadily increasing global deflections and due to the inability of the test setup to increase

Failed flange

Carbon-fiber-reinforced polymer (CFRP) grid rupture

Figure 3. Specimen DT1 failure.

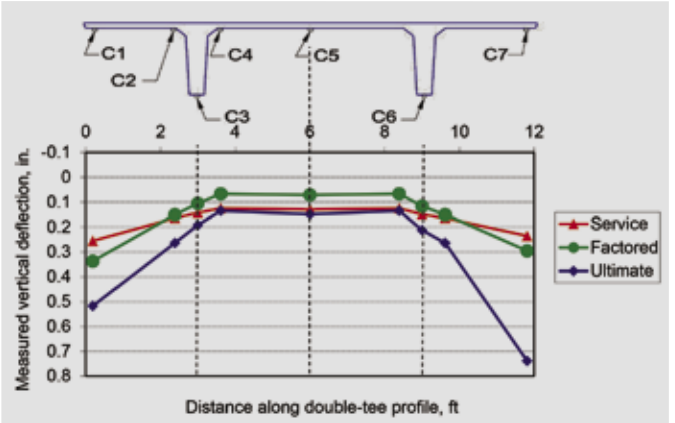

Figure 4. Deflection profile at midspan for specimen DT1. Note: C1 to C7 are the vertical deflection measurement locations across the cross section from the tip of one flange to the tip of the other. 1 in. = 25.4 mm; 1 ft = 0.305 m.

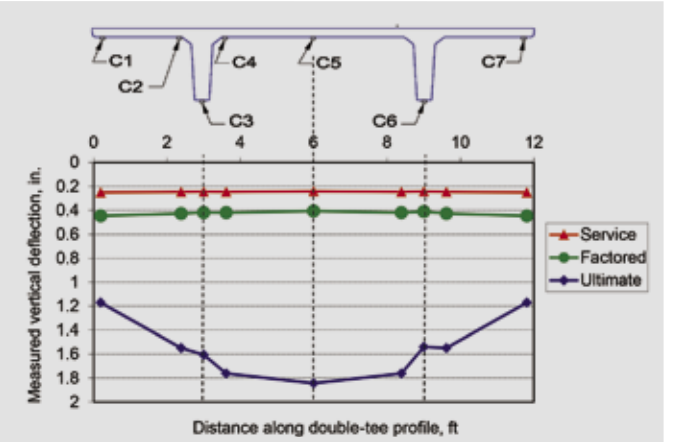

Figure 6. Deflection profile at midspan for specimen DT2. Note: 1 in. = 25.4 mm; 1 ft = 0.305 m.

the applied load further. This result indicates that the flange was capable of carrying an applied load of at least 203 lb/ft^2, which is 1.9 times the full factored design load. The maximum applied uniform pressure of 203 lb/ft^2 was maintained for approximately 10 minutes, during which time the double tee continued to deflect globally under constant load, indicating likely yielding of the longitudinal prestressing strands.

At the conclusion of the test of specimen DT2, the specimen was visually inspected for cracks. No cracks were observed in the top or bottom surface of the flanges or on either side of both stems. Specimen DT2 was entirely intact and visibly undamaged in any way at the conclusion of testing to nearly twice the factored flange design load. It is assumed that residual prestressing was sufficient to close flexural cracks in the stems that certainly would have developed under load.

Figures 6 and **7** show the measured net deflection profile at midspan and measured concrete strains for specimen DT2, respectively. The measured load-deflection behavior indicates small deflections at the service and factored load levels and confirms that the flange remained nearly flat, even at the factored load. As the load increased beyond the factored level, the deflection at the midspan increased compared with the end of the cantilever. The deflection profile for specimen DT2 indicates global deformation of the flange beyond the factored load. The measured concrete strains (Fig. 7) remained below 500 microstrain, and the load-strain behavior was relatively linear up to the maximum applied pressure with no evidence of cracks.

Comparing the behavior of the two specimens indicates the significant effect of flange thickness on both the load-carrying capacity and on global and local deflection of the double tees. Specimen DT1 highlights the concern of brittle flange failure occurring at a load less than 1.8 times the factored load,[11] and thus, the design of specimen DT1 should not be used. In final service, specimen DT1 would include a composite reinforced topping that would likely eliminate the potential for a brittle flange failure mode. However, the global brittle failure under the construction loading at a level below 1.8 times the factored load (as recommended by Lunn et al.) indicates that the design of specimen DT1 is not sufficient. Specimen DT2 illustrates how global brittle flange failure can be avoided by successfully designing for a ductile global mechanism to control.

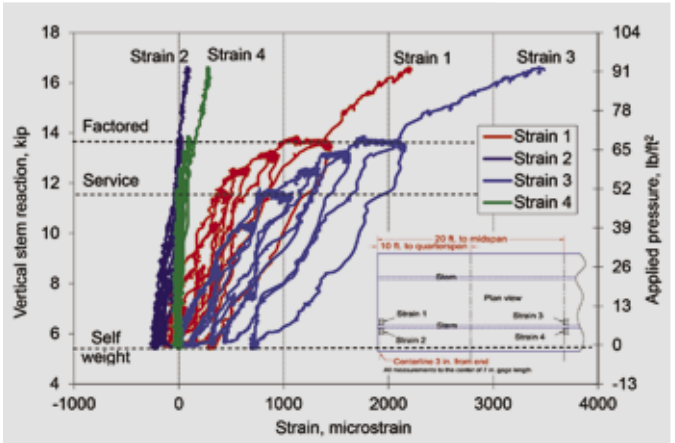

Figure 5. Measured strains for specimen DT1. Note: 1 kip = 4.448 kN; 1 lb/ft^2 = 0.0479 kPa.

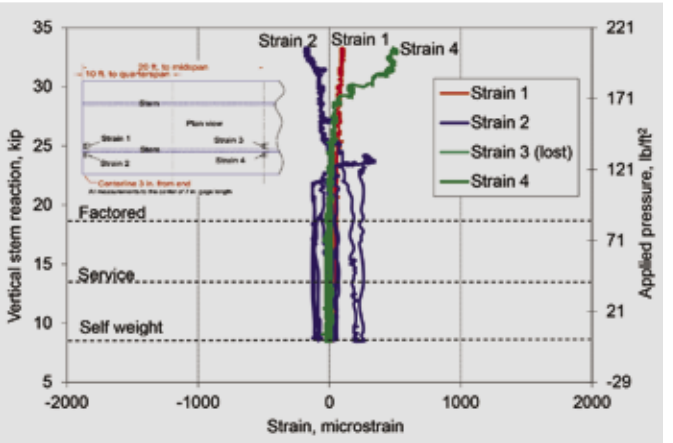

Figure 7. Measured strains for specimen DT2. Note: 1 kip = 4.448 kN; 1 lb/ft^2 = 0.0479 kPa.

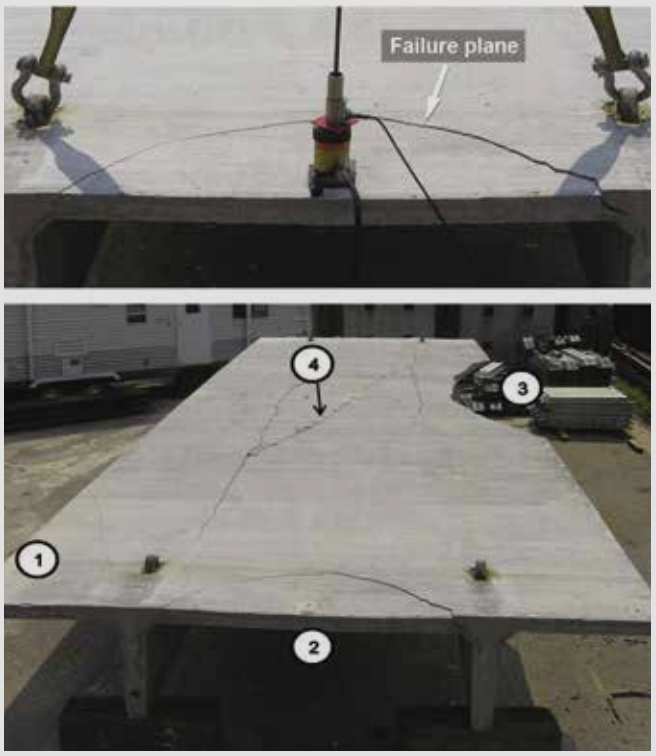

Figure 8. Test setup and cracking patterns of concentrated load tests for specimen DT2.

Concentrated load tests

According to the *PCI Design Handbook: Precast and Prestressed Concrete*,[12] precast concrete double-tee flanges should be designed to resist concentrated loads at various locations on the surface. Because specimen DT2 remained entirely intact after uniform loading, additional concentrated load tests were conducted to evaluate the behavior of the flange at various locations on the surface of the tee. Concentrated flange loads would commonly be caused in a parking structure by a vehicle jack and can sometimes control the flange design. The concentrated loads were applied through 4.5 × 4.5 in. (114 × 114 mm) steel plates bearing directly on the flange surface. Tests were conducted at the edge, midwidth of the flange at the end, and midspan section of the beam using a simple test setup. **Figure 8** shows the typical test setup and failure patterns at various tested locations. **Table 3** summarizes the measured failure loads and observed failure modes for the concentrated load tests by location of loading. The numbers shown in Fig. 8 correspond to the test numbers given in Table 3.

Table 3. Concentrated load results for specimen DT2

Test location	Failure load, lb	Failure mode
1. End of double tee, corner of flange	2530	Flexure
2. End of double tee, center of flange	11,300	Punching
3. Midspan of double tee, edge of flange	8170	Flexure
4. Midspan of double tee, center of flange	22,190	Flexure

Note: 1 lb = 4.448 kN.

Tests conducted on isolated edges of the flange do not simulate the typical conditions in the field. Typically, double-tee flanges are welded together at discrete points along the span. Accordingly, concentrated loads applied on the flange are resisted by the connected flanges of the adjacent double tees, resulting in higher failure loads and different failure surfaces. Study of typical concentrated load behavior requires testing connected double tees to determine the structural mechanism and the failure surfaces under the effect of concentrated loads.

To study the influence of connected tee flanges, it was decided to perform additional tests in the yard of a precast concrete facility on full-scale 12 × 60 ft (3.7 × 18 m) double tees. This field testing program was designed to evaluate the behavior of adjacent, connected, CFRP-reinforced double-tee flanges, as well as free double-tee edges subjected to concentrated loads. The double-tee members were connected by welding embedded flange connections located every 6 ft (1.8 m) along the length of the beam. **Figure 9** shows the two types of flange connections (one straight and one twisted) used in the field testing program.

All prestressed concrete double tees used in the field testing portion of this program were 12 × 60 ft (3.7 × 18 m). The total depth for each beam was 29.5 in. (750 mm), including a 3.5 in. (89 mm) thick flange. Each beam was prestressed longitudinally by ten ½ in. (13 mm) diameter special strands. The specified nominal compressive strength of the concrete was 6000 psi (41 MPa); however, the measured concrete strength using 4 × 8 in. (100 × 200 mm) cylinders cast and cured with the test specimens was 9000 psi (62 MPa) on the day of testing. The double-tee flanges were reinforced with a continuous sheet of CFRP grid with carbon-fiber strands spaced at 3 in. (75 mm). Five individual strands cut from the grid exhibited an average maximum tensile strength per CFRP strand of 645 lb (2870 N).

The CFRP grid was the only transverse flange reinforcement, with the exception of two no. 3 (10M) steel reinforcing bars placed at each end of the beam and a welded chord detail consisting of two no. 5 (16M) bars placed at one end only. The steel bars and chord detail are typical of all specimens (**Fig. 10**). A total of six double tees were tested in connected pairs, while only two double tees were tested individually. A total of 48 tests were performed.

Tests were conducted by applying concentrated loads at selected locations on the top surface of the flange using a hydraulic jack and self-reacting frame (**Fig. 11**). The jack was secured to the reaction beam, and the entire frame could be moved along the length of the specimens. The double tees were supported on randomly oriented fiber

Figure 9. The two types of flange connectors used in the program.

bearing pads at each end and were elevated off the ground with concrete blocks.

Specimens were tested individually or in connected pairs. **Table 4** summarizes the configurations of the 48 tests. Specimens tested in pairs were welded together at their discrete flange connections and at the chord connection. The location of the chord connection with respect to each test is designated by a dotted line on the sketches in Table 4. After conducting tests on the pair at the connected edges, the double tees were separated, rotated, and their remaining intact edges welded together to conduct the additional tests (Table 4). Locations of the applied concentrated loads are shown as open circles in the table, and each test is designated by a number and a letter. Letters A and B indicate similar locations on the adjacent flanges. For each critical location, at least four data points were measured to provide replicate data. The shaded areas on each sketch represent the locations of preexisting failures from prior tests in previous configurations.

Figure 10. Typical steel bars (both ends of the double tee) and chord detail (one end of the double tee).

For all tests, the applied load was measured by an electronic load cell. The load was applied by a hydraulic jack through a spherical bearing connection to a 4.5 × 4.5 × 1 in. (114 × 114 × 25 mm) steel plate bearing on a 4.5 × 4.5 × 0.5 in. (13 mm) neoprene pad. For selected specimens, the vertical deflection of the flange was measured during each test with string potentiometers placed directly under the applied load.

For the connected double tees, two types of loading were considered at the joint. In the first, the concentrated load was applied with the loading plate entirely set on one side of the gap and was referred to as side-of-gap loading. In the second, the loading plate was placed to span the gap and was referred to as *spans gap*. **Figure 12** illustrates the difference between the two load configurations.

Test results and discussion

The failure modes observed for the flanges of the double tees were either a flexure failure or a punching shear failure. All failures occurred in a sudden fashion. **Table 5** summarizes the results of all tests by the location of load-

Figure 11. Concentrated load test setup (two double tees welded together).

Table 4. Summary of concentrated load tests for connected flanges

Configuration	Plan view	Connection	Tests
Setup 1 DT001.1 and DT001.2 Six tests	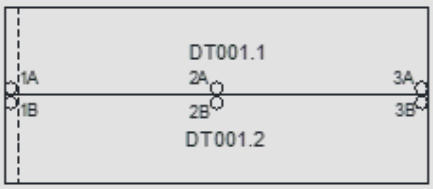	Type I	1A, 1B, 2A, 2B, 3A, 3B
Setup 2 DT003.1 and DT003.2 Six tests	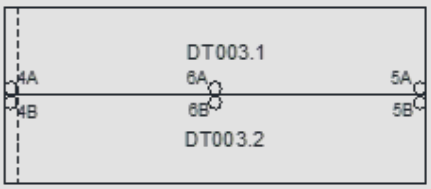	Type II	4A, 4B, 5A, 5B, 6A, 6B
Setup 3 Reuse DT001.1 and DT001.2 Five tests	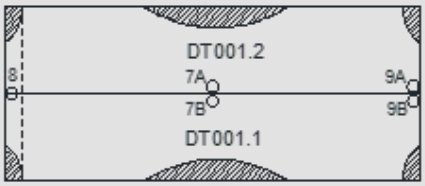	Type I	7A, 7B, 8, 9A, 9B
Setup 4 Reuse DT003.1 and DT003.2 Nine tests	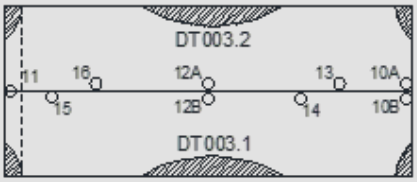	Type II	10A, 10B, 11, 12A, 12B, 13, 14, 15, 16
Setup 5 DT001.3 and DT001.4 Five tests	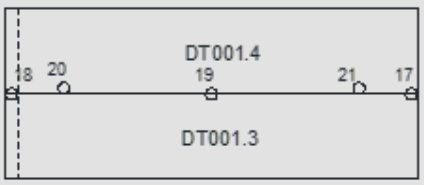	Type I	17, 18, 19, 20, 21
Setup 6 Reuse DT001.3 and DT001.4 Five tests	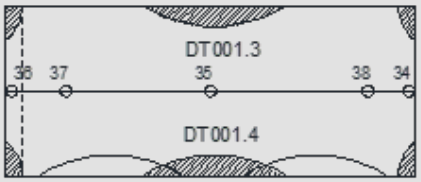	Type I	34, 35, 36, 37, 38
Setup 7 DT002.1 Six tests	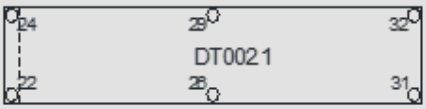	None	22, 24, 26, 29, 31, 32
Setup 8 DT002.2 Six tests	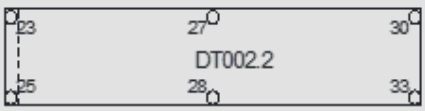	None	23, 25, 27, 28, 30, 33

One side of the gap

Spanning the gap

Figure 12. Loading plate for connected double tees.

ing. **Figure 13** shows photos of the observed failure modes for selected tests listed in Table 5.

Connected flanges loaded at internal corner locations with the load beside the gap (Fig. 13, test 1A) failed due to formation of an inclined flexure crack on the top surface of the loaded flange. This inclined crack extended from the web-flange juncture to the connector plate joining the two flanges. A portion of the concentrated load was also carried by the adjacent flange because it is connected to the loaded flange; however, failure took place in the loaded flange only, and the adjacent flange remained intact after the test.

Loading the two flanges simultaneously at an internal corner in the configuration, referred to as *spans gap*, resulted in a flexure failure in the two flanges. Failure occurred after the formation of inclined flexure cracks on the top surfaces of the two connected flanges. These cracks extended from the web-flange juncture to the connector plate for each flange (Fig. 13, test 11).

Test results for a free double tee loaded at the corner indicated failure due to formation of an inclined flexure crack on the top surface of the flange. This crack extended from the web-flange juncture to the edge of the flange with an inclination of about 60 degrees. The top right of Fig. 13, test 32, shows the failure mode for a corner test of a free double tee.

Comparing similar pairs of corner tests in Table 5 indicated that the presence of the welded chord steel at the corners of the double tees increased the ultimate capacity by 43% in some cases. For the connected double tees, the location of the load with respect to the joint (on one side of the gap or spanning the gap) had a significant effect on the ultimate capacity of the flange. In some cases, the failure load for the configuration with the load spanning the gap was 58% higher than when the load was placed on one side of the gap. Comparing the corner test results of connected double tees and free double tees indicated that the concentrated load-carrying capacity of internal corners of connected double tees was higher than that of a free double tee. The percentage increase varied from 20% to 110% depending on the type of flange connector and loading configuration (on one side of the gap or spanning the gap). This behavior is attributed to the fact that the concentrated load is resisted by the two flanges in the case of connected double tees, which results in a higher load-carrying capacity.

Test results for connected flanges loaded at the midspan with the load spanning the gap (Fig. 13, test 19) indicated flexure failure in the two flanges. The flexural cracks that constituted failure occurred immediately after reaching the cracking capacity of the flanges at the critical section. The cracks took place on the top surface of the flanges close to the web-flange juncture. Under the applied load, the cracks widened and propagated longitudinally and transversely toward the gap between the two flanges. For each of the connected flanges, the flexure crack intersected the edge of the flange beside the gap at two points almost 25 ft (7.6 m) apart. This behavior resulted in the complete detachment of segments of the two connected flanges upon rupture of the CFRP grid. In general, the failure was brittle and occurred immediately after the formation of the flexure cracks.

Test results for connected flanges loaded at the midspan with the load placed at one side of the gap exhibited a different failure mode. Figure 13, test 2B, 7A, and 12A and 12B show the failure mode for the midspan side-of-gap tests, where the observed failure was a local punching shear failure in the flange at the location of the applied load. The failure took place suddenly. In some tests, a flexure crack occurred on the top surface of the flange close to the web-flange juncture before the punching failure of the flange.

Table 5. Concentrated load test results for connected flanges

Test	Test description	Test configuration	Connectors	Load location	Load point	Load, lb	Average	Failure mode
5A	Tests of corners without chord steel	Connected double tees	Type II	Internal corner	Side of gap	3900	3326	Flexure
5B						3300		Flexure
10A						3080		Flexure
10B						3024		Flexure
9A			Type I	Internal corner	Side of gap	2600	2898	Flexure
9B						2800		Flexure
3A						3294		Flexure
3B						2897		Flexure
17					Spans gap	6100	4600	Flexure
34						3100		Flexure
30		Free double tees	None	Free corner	n/a	2700	2763	Flexure
33						3100		Flexure
31						2800		Flexure
32						2453		Flexure
1A	Tests of corners with chord steel	Connected double tees	Type I	Internal corner	Side of gap	4310	4140	Flexure
1B						3970		Flexure
4A			Type II			3400	3800	Flexure
4B						4200		Flexure
8			Type I	Internal corner	Spans gap	6200	6166	Flexure
18						6900		Flexure
36						5400		Flexure
11			Type II			6000	6000	Flexure
22		Free double tees	None	Free corner	n/a	2800	2821	Flexure
24						3264		Flexure
23						2638		Flexure
25						2580		Flexure
2A	Tests between connectors at midspan	Connected double tees	Type I	Midspan	Side of gap	14,800	15,333	Punching
7A						14,952		Punching
7B						16,079		Punching
2B						15,500		Punching
6A			Type II			14,500	13,875	Flexure
6B						12,600		Punching
12A						14,600		Punching
12B						13,800		Punching
19			Type I		Spans gap	19,442	17,521	Flexure
35						15,600		Flexure
26	Tests of free edges at midspan	Free double tees	None	Midspan (edge)	n/a	9595	9347	Flexure
29						9778		Flexure
27						9773		Flexure
28						8240		Flexure
15	Tests at connector	Connected double tees	Type II	Second connector	Side of gap	12,521	13,364	Flexure
13				Fourth connector		14,630		Flexure
20			Type I	Second connector		11,956		Flexure
21				Fourth connector		12,023		Flexure
16			Type II	Fourth connector		15,066		Flexure
14				Fourth connector		13,985		Flexure
37			Type II	Second connector	Spans gap	13,800	13,400	Flexure
38				Second connector		13,000		Flexure

Note: n/a = not applicable. 1 lb = 4.448 N.

Test 1A: Connected double tees, internal corner, side of gap

Test 11: Connected double tees, internal corner, spans gap

Test 32: Free double tee, corner

Test 19: Connected double tees, midspan, spans gap

Test 2B: Connected double tees, midspan, side of gap

Test 7A: Connected double tees, midspan, side of gap

Tests 12A and 12B: Connected double tees, midspan, side of gap

Test 28: Free double tee, midspan, edge

Test 38: Test at connector

Figure 13. Failure modes for selected load tests given in Table 4.

Test results for a free double tee with loading at the midspan edge (Fig. 13, test 28) indicated a flexural failure in the flange. Failure occurred after the formation of a longitudinal flexural crack on the top surface of the flange. This crack initiated close to the web-flange juncture and progressed longitudinally and transversely toward the edge of the flange. The failure resulted in complete detachment of a segment of the flange upon rupture of the CFRP grid.

Results of tests conducted directly over connectors indicated a flexural failure in the two connected flanges. Failure occurred immediately after the formation of flexural cracks on the top surface of the two flanges. The cracks initiated close to the web-flange juncture and propagated in the longitudinal and transverse directions toward the gap between the two flanges (Fig. 13, test 38).

In general, the load-carrying capacity of the flange at midspan for connected double tees was higher than that of the free double tee. For example, the load-carrying capacity of the connected flanges at the midspan (test 19 in Table 5) was almost twice that of a free flange at same location,

test 26. The case of connected double tees more closely matches the real conditions in parking structures, where double tees are connected using welded joints.

For a connected pair of double tees, the corner locations are the most critical locations with the least load-carrying capacity compared with the midspan locations. Test results indicated that the ultimate capacity of the flange at a midspan location exceeded the capacity at an internal corner location up to five times in some cases. Results of tests conducted directly over the connectors indicated that the two types of connectors considered in this study provided almost equivalent strengths at all tested locations.

In general, concentrated load test results indicated that the failure load and mode of failure were highly influenced by the test configuration, load location, and presence of chord steel. **Figure 14** shows the measured load compared with the vertical displacement under the load for selected tests at the corner and midspan locations.

Idealized failure surfaces and design methodology

Results of the concentrated load tests conducted on the double tees in the field testing program were used to develop idealized failure surfaces at various locations of the double-tee flange. The idealized failure surfaces were developed based on the crack patterns observed in the tests.

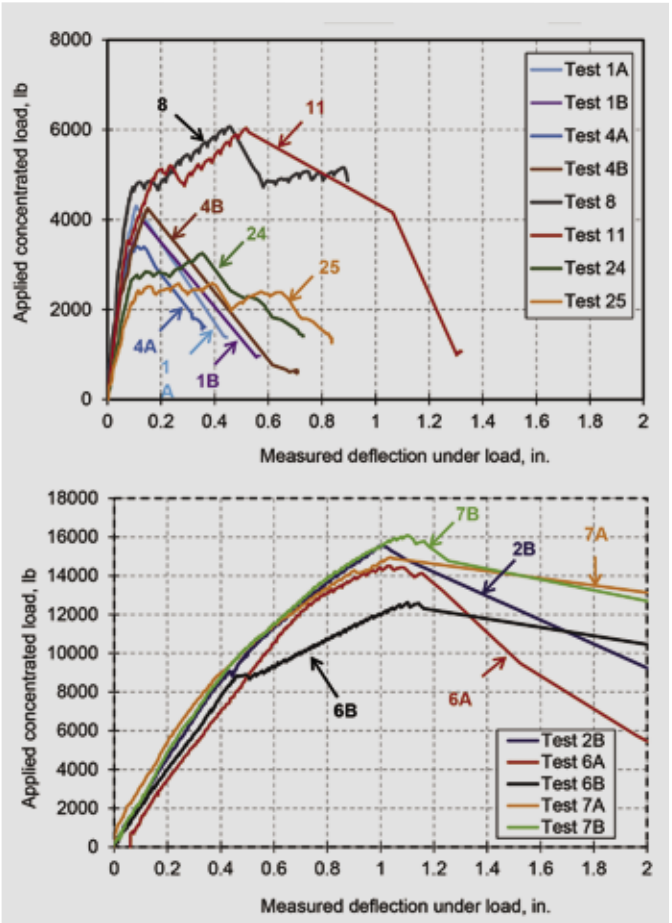

Figure 14. Load deflection for selected tests. Note: 1 in. = 25.4 mm; 1 lb = 4.448 N.

Figure 15 shows the idealized failure surfaces for a corner location and a location at any point along the edge of a free flange sufficiently far from an end or other discontinuity. **Figure 16** shows the idealized failure surfaces and mode of failure for the internal corner and midspan locations of connected double tees for the cases of the load placed at one side of the gap and spanning the gap.

The nominal moment capacity of the flange M_n was determined using the method recommended by the American Concrete Institute's (ACI's) *Guide for the Design and Construction of Structural Concrete Reinforced with FRP Bars* (ACI 440.1R-06).[13] According to this method, if the FRP reinforcement ratio ρ_f, calculated using Eq. (1), is less than the balanced FRP reinforcement ratio ρ_{fb} from Eq. (2), failure is likely due to rupture of the FRP before crushing of the concrete. In this case, a simplified and conservative method recommended by ACI 440.1R-06 was used to determine the nominal moment capacity M_n, as given by Eq. (3).

$$\rho_f = \frac{A_f}{bd} \tag{1}$$

where

A_f = area of FRP reinforcement

b = width of the flange

d = effective depth of the reinforcement

$$\rho_{fb} = 0.85\beta_1\left(\frac{f_c'}{f_{fu}}\right)\left(\frac{E_f\varepsilon_{cu}}{E_f\varepsilon_{cu}+f_{fu}}\right) \tag{2}$$

where

β_1 = factor relating the depth of the equivalent rectangular compressive stress block to the neutral axis depth, as specified by ACI's *Building Code Requirements for Structural Concrete (ACI 318-14) and Commentary (ACI 318R-14)*[14]

f_c' = concrete compressive strength at 28 days

f_{fu} = rupture stress of the FRP

E_f = modulus of elasticity of the FRP

ε_{cu} = concrete crushing strain

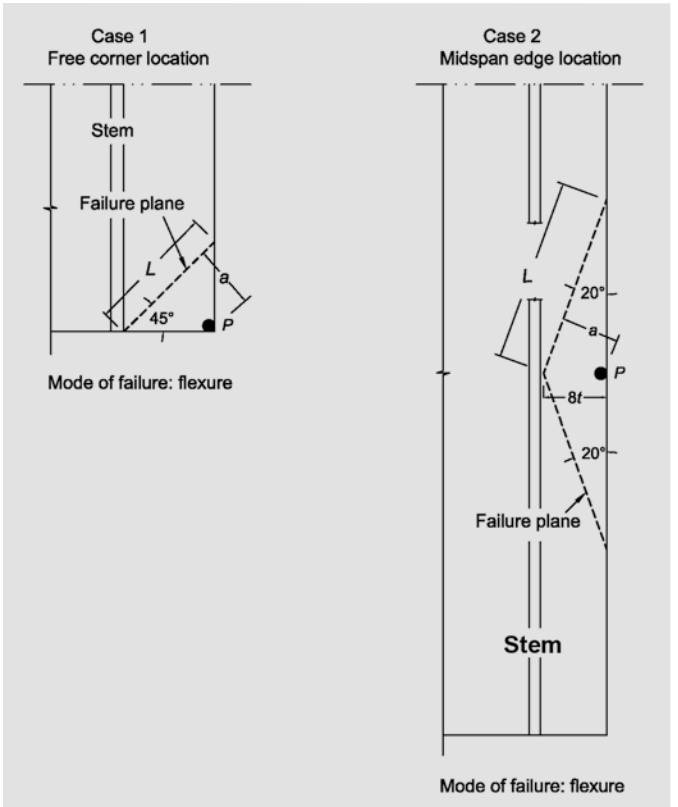

Figure 15. Idealized failure surfaces for free flange. Note: a = lever arm; L = length of failure plane; P = applied concentrated load; t = thickness of flange.

$$M_n = A_f f_{fu}\left[d - \beta_1\left(\frac{c_b}{2}\right)\right] \quad (3)$$

where

c_b = distance from the extreme compression fiber to the neutral axis at the balanced strain condition, as determined by Eq. (4)

$$c_b = \left(\frac{\varepsilon_{cu}}{\varepsilon_{cu} + \varepsilon_{fu}}\right)d \quad (4)$$

where

ε_{fu} = rupture strain of the FRP

The experimental results of this study indicated that for most of the tests, ultimate failure was controlled by the flexural cracking capacity of the flange rather than the FRP reinforcement ratio. This was also indicated by calculations because the cracking moment of the flange M_{cr} exceeds the nominal flexural moment corresponding to the tensile rupture strength of the FRP M_n. The cracking moment M_{cr} can be determined using Eq. (5).

$$M_{cr} = \frac{f_r b t^2}{6} \quad (5)$$

where

f_r = modulus of rupture = $7.5\sqrt{f_c'}$, as specified by ACI 318-14

t = thickness of the flange

The observed idealized failure surfaces and the cracking capacity of the flange M_{cr} were used to determine the nominal concentrated load-carrying capacity of the flange P_n at various locations of the double-tee flange as illustrated in the following design example. Due to the brittle nature of the CFRP grid at failure, it is recommended that failure modes involving flange flexure be designed such that $0.75P_n$ exceeds 1.33 times the factored design concentrated load P_u, as shown in Eq. (6) and proposed by Lunn et al.[11] for CFRP-reinforced double-tee flanges subjected to uniform loads.

$$0.75P_n > 1.33P_u \quad (6)$$

Design example

The following design example illustrates the procedure proposed for predicting the nominal concentrated load-carrying capacity of the flange P_n at various locations for free and connected double-tee flanges. For a CFRP grid with 3 in. (75 mm) spacing, a tensile strength f_{fu} of 120 ksi (827 MPa), a rupture strain ε_{fu} of 0.014, and a cross-sectional area A_f of 0.0216 in.^{2}/ft (45.8 mm^2/m), the rupture strength of FRP is 2.6 kip/ft (38 kN/m). Using a clear concrete cover of ¾ in. (19 mm) and effective depth d of 2.75 in. (69.9 mm), the reinforcement ratio ρ_f can be determined using Eq. (1).

$$\rho_f = \frac{A_f}{bd}$$

$$= \frac{0.0216}{(12)(2.75)}$$

$$= 0.00065$$

Using the measured concrete strength at 28 days f_c' as 8400 psi (58 MPa), elastic modulus of the CFRP grid E_f of 8570 ksi (59.1 MPa), and concrete crushing strain ε_{cu} of 0.003, the balanced reinforcement ratio can be determined using Eq. (2).

$$\rho_{fb} = 0.85\beta_1\left(\frac{f_c'}{f_{fu}}\right)\left(\frac{E_f\varepsilon_{cu}}{E_f\varepsilon_{cu} + f_{fu}}\right)$$

$$= (0.85)(0.65)\left(\frac{8.4}{120}\right)\left[\frac{(8570)(0.003)}{(8570)(0.003)+120}\right]$$

$$= 0.0068$$

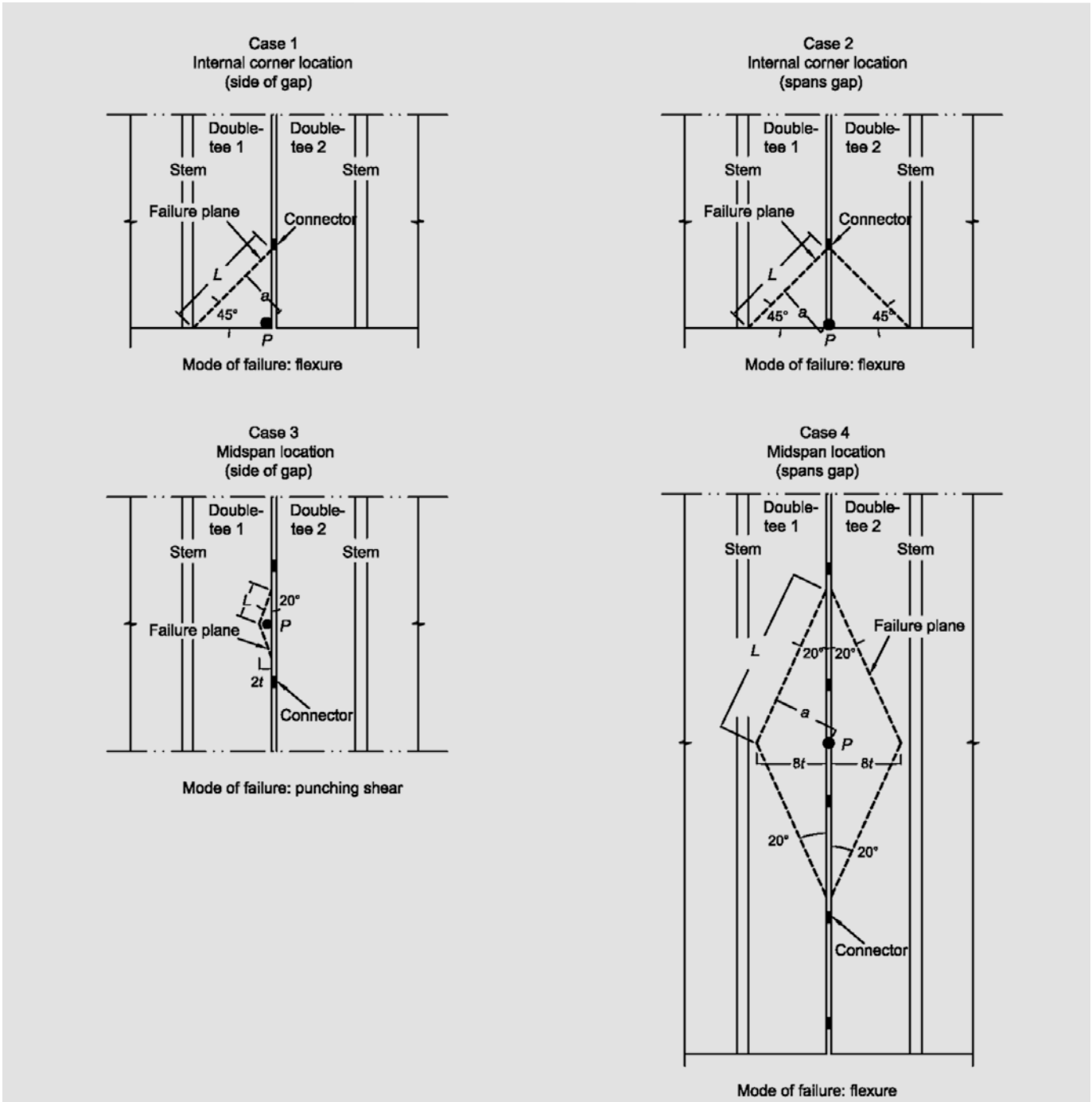

Figure 16. Idealized failure surfaces for connected flanges. Note: a = lever arm; L = length of failure plane; P = applied concentrated load; t = thickness of flange.

Because the FRP reinforcement ratio ρ_f is less than the balance ratio ρ_{fb}, the nominal moment capacity of the flange M_n can be determined based on the conservative estimation of depth of the compression zone for the balanced section c_b using Eq. (3) and (4).

$$c_b = \left(\frac{\varepsilon_{cu}}{\varepsilon_{cu} + \varepsilon_{fu}}\right) d$$

$$= \left(\frac{0.003}{0.003 + 0.014}\right) 2.75$$

$$= 0.485 \text{ in. } (12.4 \text{ mm})$$

$$M_n = A_f f_{fu}\left(d-\beta_1\frac{c_b}{2}\right)$$
$$= (0.0216)(120)\left[2.75-0.65\left(\frac{0.485}{2}\right)\right]$$
$$= 6.7 \text{ kip-in./ft (2.48 kN-m/m)}$$

The cracking moment capacity of the flange M_{cr} can be determined using Eq. (5).

$$M_{cr} = \frac{f_r b t^2}{6}$$
$$= \frac{(7.5)\left(\sqrt{8400}\right)(12)(3.5)^2}{6(1000)}$$
$$= 16.8 \text{ kip-in./ft (6023 kN-m/m)}$$

The analysis indicated that the cracking moment capacity M_{cr} exceeds the nominal flexural moment M_n. Therefore, the flexural capacity of the flange is controlled by the cracking moment and should be used to predict the concentrated load-carrying capacity of the flange P_n at the proposed failure surfaces for the free and connected double-tee flanges.

Case 1: Load spanning the gap at the corner of connected flanges

The proposed failure mode for this case is flexure along the proposed failure surface (Fig. 16, top row, right).

Assume that the load is shared equally by the two flanges; therefore, the load acting on each flange is $P_n/2$. The length of the failure plane L can be determined based on the 30 in. (760 mm) cantilever length of the flange.

L = 30/cos 45

= 42.4 in. (1080 mm)

The lever arm a can be determined as:

a = (30)sin 45

= 21.2 in. (538 mm)

Using the cracking moment capacity M_{cr} along the length L, the nominal concentrated load P_n can be determined.

$$M_{cr}L = \frac{P_n}{2}a$$
$$(16.8)\left(\frac{42.4}{12}\right) = \frac{P_n}{2}(21.2)$$
$$P_n = 5.6 \text{ kip (25kN)}$$

This value compares well with the average load of 6 kip (27 kN) measured for five tests.

Case 2: Load spanning the gap at midspan of connected flanges

The proposed failure mode for this case is flexure along the failure surface (Fig. 16, bottom row, right).

Similarly, assuming that the load is equally shared by the two flanges, the load acting on each flange is $P_n/2$.

The dimensions of the failure surface are as follows:

t = thickness of flange

= 3.5 in. (89 mm)

L = 8t/sin 20

= 81.8 in. (2080 mm)

The lever arm a can be determined based on the proposed failure surface.

a = 8t/cos 20

= 26.3 in. (668 mm)

The nominal load can be determined as follows:

$$\frac{P_n}{4}a = M_{cr}L$$
$$\frac{P_n}{4}(26.3) = (16.8)\left(\frac{81.8}{12}\right)$$
$$P_n = 17.4 \text{ kip (77.8 kN)}$$

This value compares well with the average load of 17.5 kip (77.8 kN) measured for two tests.

Case 3: Load at one side of the flange at midspan of the connectors

The proposed failure mode for this case is a punching shear failure along the failure surface (Fig. 16, bottom row, left). Using a nominal concrete shear strength of $\sqrt{f_c'}$, the nominal load P_n can be determined based on the flange thickness t and the length of the failure plane L.

t = 3.5

L = 2t/sin 20

= 20.4 in. (518 mm)

$$P_n = \sqrt{f_c'}\,(2Lt)$$

$$= \frac{\sqrt{8400}\,(2)(20.4)(3.5)}{1000}$$

$$= 13.0 \text{ kip (58kN)}$$

The predicted value also compares well with the average load of 14.6 kip (64.9 kN) measured for seven tests.

Case 4: Load at the corner of the free flange

The proposed failure mode for this case is flexure along the proposed failure surface (Fig. 15, left). The length of the failure plane L can be determined:

$$L = 30/\cos 45$$

$$= 42.4 \text{ in. (1080 mm)}$$

$$a = (30)\sin 45$$

$$= 21.2 \text{ in. (538 mm)}$$

$$P_n a = M_{cr} L$$

$$P_n(21.2) = (16.8)\left(\frac{42.4}{12}\right)$$

$$P_n = 2.8 \text{ kip (12kN)}$$

The predicted value also compares well with the average load of 2.8 kip (12 kN) measured for eight tests.

Case 5: Load at midspan of the free flange

The proposed failure mode for this case is flexure along the proposed failure surface (Fig. 15, right). From the geometry of the failure surface:

$$t = 3.5 \text{ in. (89 mm)}$$

$$L = 8t/\sin 20$$

$$= 81.8 \text{ in. (2080 mm)}$$

$$a = 8t/\cos 20$$

$$= 26.3 \text{ in. (668 mm)}$$

The load carried by each segment of the failure surface is $P_n/2$.

$$\frac{P_n}{2} a = M_{cr} L$$

$$\frac{P_n}{2}(26.3) = (16.8)\left(\frac{81.8}{12}\right)$$

$$P_n = 8.7 \text{ kip (39kN)}$$

The predicted value compares well with the average load of 9.3 kip (41 kN) measured for four tests.

Conclusion

Based on this study, the following conclusions and recommendations may be drawn:

- CFRP grid can be used effectively for transverse flange reinforcement in precast, prestressed concrete double tees, as demonstrated by the test of specimen DT2, where ductile global behavior prevented brittle global flange failure.
- When flange failures developed in the tested beams, they were brittle, with failure of the CFRP grids often corresponding to concrete cracking; however, failure loads were always substantially higher than the specified factored loads.
- The global flange failure of specimen DT1, though occurring at a load in excess of the factored level, indicates that the design of specimen DT1 should not be used.
- When flange flexure failures are possible, designs with CFRP grid should be performed so that three-quarters of the nominal load capacity equals or exceeds 1.3 times the factored design load as described by Lunn et al.[11] This method provides an equivalent capacity of at least 1.8 times the factored load, which for typical designs should correspond to a total safety factor against flange failure of about 3.0. Such high levels of overstrength should be sufficient to prevent brittle flange failures by allowing ductile global mechanisms to control.
- The concentrated load-carrying capacity and failure surface of flanges reinforced with CFRP grids depends highly on the location of the applied concentrated load. In most cases, concentrated loads are resisted by a flange bending mechanism; however, a punching shear mechanism should also be checked.
- The concentrated load-carrying capacity of a connected pair of double tees is substantially higher than the capacity of a free double-tee edge or corner. Therefore, connections play an important role in the concentrated load capacity of double-tee flanges. Both types of tested connections exhibited similar behavior.
- For connected double tees, the location of the concentrated load with respect to the joint had a significant effect on the ultimate capacity of the flange. Flange capacities were higher when loads were applied across the joint than directly beside the joint, demonstrating

that the flange connections are not 100% effective at transferring load from flange to flange.

- Idealized failure surfaces at various tested locations were proposed for the free and connected flanges tested, and simple calculation methods were shown to be effective at predicting the concentrated load-carrying capacity of the flange.

Acknowledgments

The authors would like to thank AltusGroup Inc. for supporting this research effort. They would also like to thank Metromont Corp. for supporting the field trial at its Richmond, Va., facility. In addition, the authors are grateful to the staff and students at the Constructed Facilities Laboratory at North Carolina State University for their help throughout the experimental program. In particular, Johnathan McEntire was instrumental in the field testing program and should be commended for his efforts.

References

1. Rizkalla, S., and G. Tadros. 1994. "A Smart Highway Bridge in Canada." *Concrete International* 16 (6): 42–44.

2. Rizkalla, S., E. Shehata, A. Abdelrahman, and G. Tadros. 1998. "A New Generation: Design and Construction of a Highway Bridge with CFRP." *Concrete International* 20 (6): 35–38.

3. Pessiki, S., and A. Mlynarczyk. 2003. "Experimental Evaluation of Composite Behavior of Precast Concrete Sandwich Wall Panels." *PCI Journal* 48 (2): 54–71.

4. Frankl, B., G. Lucier, T. Hassan, and S. Rizkalla. 2011. "Behavior of Precast, Prestressed Concrete Sandwich Wall Panels Reinforced with CFRP Shear Grid." *PCI Journal* 56 (2): 42–54.

5. Sopal, G., S. Rizkalla, and L. Sennour. 2013. "CFRP Grid for Concrete Sandwich Panels." In *Proceeding of the 2013 Asia-Pacific Conference on FRP in Structures (APFIS 2013), Melbourne, Vic., Australia, December 11-13*. Melbourne, Australia: International Institute for FRP in Construction.

6. Naito, C., J. Hoemann, M. Beacraft, and B. Bewich. 2012. "Performance and Characterization of Shear Ties for Use in Insulated Precast Concrete Sandwich Wall Panels." *ASCE Journal of Structural Engineering* 138 (1): 52–61.

7. Banthia, N., M. Al-Asaly, and S. Ma. 1995. "Behavior of Concrete Slabs Reinforced with Fiber-Reinforced Plastic Grid." *Journal of Materials in Civil Engineering* 7 (4): 252–257.

8. Matthys, S., and L. Taerwe. 2000. "Concrete Slabs Reinforced with FRP Grids. II: Punching Resistance." *Journal of Composites for Construction* 4 (3): 154–161.

9. El-Gamal, S., E. El-Salakawy, and B. Benmokrane. 2005. "Behavior of Concrete Bridge Deck Slabs Reinforced with Fiber-Reinforced Polymer Bars under Concentrated Loads." *ACI Structural Journal* 102 (5): 727–735.

10. CAN/CSA-S6-14. 2015. *Canadian Highway Bridge Design Code*. Rexdale, ON, Canada: Canadian Standard Association.

11. Lunn, D., G. Lucier, S. Rizkalla, N. Cleland, and H. Gleich. 2015. "New Generation of Precast Concrete Double Tees Reinforced with Carbon-Fiber-Reinforced Polymer Grid." *PCI Journal* 60 (4): 37–48.

12. PCI Industry Handbook Committee. 2010. *PCI Design Handbook: Precast and Prestressed Concrete*. MNL-120. 7th ed. Chicago, IL: PCI.

13. ACI (American Concrete Institute) Committee 440. 2006. *Guide for the Design and Construction of Structural Concrete Reinforced with FRP Bars*. ACI 440.1R-06. Farmington Hills, MI: ACI.

14. ACI Committee 318. 2014. *Building Code Requirements for Structural Concrete (ACI 318-14) and Commentary (ACI 318R-14)*. Farmington Hills, MI: ACI.

Notation

a = lever arm measured from the applied concentrated load perpendicular to the failure plane

A_f = area of fiber-reinforced polymer reinforcement

b = width of the flange

c_b = distance from the extreme compression fiber to the neutral axis at the balanced strain condition

d = effective depth of the reinforcement

DL = dead load

E_f = modulus of elasticity of the fiber-reinforced polymer

f_c' = concrete compressive strength at 28 days

f_{fu} = rupture stress of the fiber-reinforced polymer

f_r = modulus of rupture for concrete = $7.5\sqrt{f_c'}$

L = length of failure plane

LL = live load

M_{cr} = cracking moment of the flange

M_n = nominal moment capacity of the flange

P = applied concentrated load

P_n = nominal concentrated load-carrying capacity of the flange

P_u = factored design concentrated load

SL = snow load

t = thickness of the flange

β_1 = factor relating the depth of the equivalent rectangular compressive stress block to the neutral axis depth

ε_{cu} = concrete crushing strain

ε_{fu} = rupture strain of the fiber-reinforced polymer

ρ_f = fiber-reinforced polymer reinforcement ratio

ρ_{fb} = balanced fiber-reinforced polymer reinforcement ratio

About the authors

Amir W. Botros, PhD, is a former doctoral student in the Civil, Construction and Environmental Engineering Department at North Carolina State University (NCSU) in Raleigh. He earned his BS and MS from Ain Shams University in Cairo, Egypt. He is an engineer in training at SDR Engineering Consultants Inc. in Tallahassee, Fla.

Gregory W. Lucier is a research assistant professor in the Civil, Construction and Environmental Engineering Department and also serves as the manager of the Constructed Facilities Laboratory at NCSU.

Sami H. Rizkalla, PhD, FPCI, FACI, FASCE, FIIFC, FEIC, FCSCE, is a Distinguished Professor of Civil Engineering and Construction, director of the Constructed Facilities Laboratory, and director of the NSF Center on Integration of Composites into Infrastructure at NCSU.

Harry Gleich, PE, FACI, FPCI, is vice president of engineering for Metromont Corp., serves on many PCI committees, including the Technical Activities Council, and is the immediate past chair of the PCI Research and Development Council and past chair of the PCI Precast Insulated Wall Panels Committee. At ACI he also serves on numerous committees and is the former chair of ACI Committee 533, Precast Panels, and former chair of ACI Committee 550, Precast Concrete Structures.

Abstract

This paper presents an experimental program conducted to evaluate the performance of precast concrete double-tee flanges reinforced with carbon-fiber-reinforced polymer grids under various types of loading. The experimental program comprised two different studies, with a total of 10 full-scale precast, prestressed concrete double-tee beams subjected to uniform and concentrated loads applied to the top surface of their flanges. The first study included testing two double-tee beams with 2 and 3.5 in. (50 and 89 mm) thick flanges to evaluate the behavior, including the flange bending behavior, under uniformly distributed loads using an enclosed vacuum chamber. In the second study, a total of eight double tees were tested either individually or in connected pairs to determine the load-carrying capacity of the flanges when subjected to concentrated loads applied at various points on the flange. Test results from the first study indicated that the flanges were capable of resisting a maximum applied load significantly higher than their factored design loads. Results of the second study indicated that the concentrated load-carrying capacity of the flange depends on the location of the applied load. Based on this investigation, an idealized failure surface and the corresponding mode of failure were identified for the free and connected flange of prestressed concrete double tees subjected to concentrated loads.

Keywords

Carbon-fiber-reinforced polymer grid, CFRP, concentrated loading, double tee, flange bending, flange connection, load, uniform loading.

Review policy

This paper was reviewed in accordance with the Precast/Prestressed Concrete Institute's peer-review process.

Reader comments

Please address reader comments to journal@pci.org or Precast/Prestressed Concrete Institute, c/o *PCI Journal*, 200 W. Adams St., Suite 2100, Chicago, IL 60606.